NMR structural characterization of the CDK inhibitor p19^{INK4d}

Wenzel Kalus[a], Roland Baumgartner[a], Christian Renner[a], Angelika Noegel[a], Francis Ka Ming Chan[b], Astar Winoto[b], Tad A. Holak[a,*]

[a] *Max Planck Institute for Biochemistry, D-82152 Martinsried, Germany*
[b] *Department of Molecular and Cell Biology, 469 Life Science Addition, University of California, Berkeley, CA 94720-3200, USA*

Received 1 October 1996; revised version received 27 November 1996

Abstract p19^{INK4d} is a 165 amino acid protein that belongs to the INK4 family of CDK4 and CDK6 inhibitors. Assignments of ^{1}H, ^{15}N and ^{13}C resonances have enabled the determination of the secondary structure of the protein which is largely α-helical (residues 14–18, 21–29, 54–62, 77–83, 87–95, 110–116, 120–128, 142–148 and 152–160). The protein comprises five 32-amino acid ankyrin-like repeats; each ankyrin repeat contains a helix-β-turn-helix core. The exception is the second ankyrin repeat, which lacks the first helix. All β-turns have a central glycine residue flanked by two residues in β-conformations. There is also a high conservation of Ala at position 8 in the first helix and Leu-Leu(Val) at positions 17–18 of the second helix in all ankyrin repeats of p19. The location of the helix-turn-helix segments found in p19 should be general for all other members of the INK4 family, including, for example, a homologous tumor suppressor p16^{INK4a}. ^{1}H-^{15}N heteronuclear steady-state NOE measurements on p19 indicate that most of the backbone of p19^{INK4d} exists in a well defined structure of limited conformational flexibility on the nano- to picosecond time scale.

Key words: p19; CDK inhibitor; Ankyrin repeat; INK4; Nuclear magnetic resonance

1. Introduction

The INK4 proteins constitute a family of cyclin-dependent kinase inhibitors that was discovered with the human gene product p16^{INKa} 3 years ago [1–3]. These proteins interact exclusively with the G1 cyclin D-dependent kinases CDK4 and CDK6, which phosphorylate the retinoblastoma (pRb) protein thereby enabling the cell to enter S phase [2–4]. INK4 proteins thus can limit this phosphorylation of pRb; their ectopic overexpression in proliferating cells can inhibit CDKs in vivo [5,6], induce G1 arrest [2,5–10], and revert cell transformation in normal diploid fibroblasts by *ras* and c-*myc*, but not by *ras* and adenovirus E1A [11]. In mammalian cells, there exists at least one other family of CDK inhibitors, represented by prototype CDK inhibitor p21 [2]. In contrast to p16, the p21$^{Waf1/CIP1}$ family of proteins can interact with and inhibit the activity of a wide spectrum of CDK kinases.

The INK4 family of CDK inhibitors currently contains four gene products: p16 (also known as INK4a, MTS1, CDK4I, and CDKN2 [1,12,13]), p15 (also known as MTS2, INK4b, and p14 [7,12,14]), p18 (INK4c [6,7]), and p19 (INK4d [15,16]). Tandemly linked *INK4a* and *INK4b* genes map to the short arm of human chromosome 9 and their protein products function as tumor suppressors [2,3,12,13,17–19]. By contrast, *INK4* genes encoding p18 and p19 map to other human chromosomes 1p32 and 19p13, respectively [6,7,15–17]. Similar to other INK4 proteins, p19^{INK4d} is expressed ubiquitously in proliferating cultured cells and in normal mouse tissues [6,7,15,17]. These proteins, however, have not been linked to tumor formation, evidence against strict redundancy of the INK4 proteins despite their apparently indistinguishable biochemical properties [2].

All members of the INK4 protein family contain several 32-amino acid ankyrin-like motifs which are considered to participate in protein-protein interactions [20]. The proteins are homologous to each other, with p16 and p15 having 44% identity in the first 50 amino acids and 97% identity in the last three ankyrin domains [1,14]. Mouse p19 and p18 exhibit only 40% amino acid identity to one another, and both show a similar degree of homology to human p16 and p15 [6]. In contrast, mouse p19 and p18 exhibit more than 90% amino acid identity with their human counterparts [6,15]. The human p19, the subject of our study, has a 48% identity with that of human p16 over a stretch of 130 amino acids [15,16]. There is no structural information yet available on any protein of this family. In the present report, we describe the determination of the complete secondary structure of human p19 in solution using NMR spectroscopy. ^{1}H-^{15}N heteronuclear steady-state NOE experiments were performed to further characterize p19 protein structure and stability.

2. Materials and methods

2.1. Preparation of p19

p19 was expressed and purified in BL21(DE3) (Novagen, Madison, WI, USA) as a glutathione fusion protein, using pGEX 2T (Pharmacia Biotech, Sweden) as an expression vector as described in [21]. To obtain higher expression yields of p19 in *Escherichia coli* in minimal media, the p19 gene was subcloned into the *Nde*I and *Bam*HI restriction sites of the pET15b vector (Novagen) in a frame to a His tag. PCR was used to introduce the restriction sites using following primers: 5′p19 GGGAATTCCATATG_CTGCTGGAGGAGGTTC; 3′p19 GCGGGATCC_TCACAGCGGGGCCACCAT (overhangs separated by the underscore). Conditions for the template were as follows: pGEX 2T-p19-pl; polymerase Vent (National Biolabs, UK), 2 mM $MgSO_4$; 92°C 60 s, 59°C 60 s, 72°C 45 s, 32 cycles. To verify the correctness of PCR, this construct was transformed into the *E. coli* strain *JM83* [22] to produce a plasmid used for sequencing. For expression, the construct was transformed into *E. coli* strain *BL21(DE3)pLys* (Novagen). Overnight cultures of BL21(DE3)pLys-p19 were diluted 20-fold with a fresh medium (see below). Recombinant proteins were induced with 1 mM IPTG (isopropyl-β-D-thiogalactopyranoside) at an OD of 0.9 for 2 h in full (LB) and selective media, 3 h in minimal media, and 5 h in the D_2O-medium.

2.2. ^{15}N, ^{13}C, and ^{2}H labeling

A standard LB medium was used for full media. The expression level of p19 was about 8 mg/l. The uniform ^{15}N-labeled and $^{13}C/^{15}N$-double labeled samples were prepared by growing bacteria on a M9 minimal medium containing ^{15}N-ammonium chloride (1 g/l) as the only nitrogen source [23,24] or ^{15}N-ammonium chloride (1 g/l) and

*Corresponding author. Fax: (49) (89) 8578-3777.
E-mail: Holak@vms.biochem.mpg.de

PII S0014-5793(96)01465-2

^{13}C-glucose (2 g/l) in case of double-labeled samples, supplemented with minerals and cofactors [25]. The same media was used for ^{15}N/^{3}C/^{2}D labeling, except that a 70% D_2O/30% H_2O mixture was used. The bacteria were first grown in full media to an OD of 1.0 and then diluted 1:10 to minimal medium (30% D_2O) and grown to an OD of 1.0 in order to adapt the bacteria to D_2O conditions. This solution was diluted 1:5 to the 70% D_2O minimal medium and grown to an OD of 0.5 and used to inoculate a 90% D_2O minimal overnight culture. The expression was then performed as described above for a 70% D_2O minimal medium culture. The yield of the purified protein was about 7 mg/l culture. Reverse labeling was performed in the ^{15}N minimal medium enriched with one ^{14}N-amino acid. The following reverse labeled samples were prepared using ^{14}N histidine (200 mg/l), ^{14}N asparagine (200 mg/l), ^{14}N threonine (800 mg/l), ^{14}N lysine (200 mg/l), ^{14}N methionine (200 mg/l), ^{14}N arginine (400 mg/l), and ^{14}N phenylalanine (1 g/l). For ^{15}N amino acid selective labeling, the minimal medium (^{14}N) was enriched with unlabeled amino acids and the double amount of the ^{15}N labeled amino acid [24]. Selectively labeled p19 in ^{15}N glycine/serine, leucine, valine, alanine and phenylalanine were prepared. The yield of purified protein was about 15 mg/l. Purification of the protein was performed under either native or denaturing conditions. In the native conditions, the cell pellet from a 1-l culture was resuspended in 20 ml buffer A (5 mM imidazole, 50 mM natrium phosphate, pH 8.0) and lysed using a French press. The cell solution was centrifuged at 60 000×g and 4°C for 30 min. The supernatant was loaded on a 3 ml Ni-NTA column (Qiagen, Hilden, Germany) washed with 50 ml buffer A, 100 ml buffer B (20 mM imidazole, 50 mM natrium phosphate, pH 8.0) and eluted using a 100 ml gradient comprising buffer A and buffer C (200 mM imidazole, 50 mM Na-phosphate, pH 8.0). Fractions were analyzed by SDS-PAGE and pure fractions were concentrated with Centricon 10 and dialyzed against the sample buffer S (50 mM NaCl, 50 mM KCl, 20 mM phosphate, pH 6.9). Under denaturing conditions, the cell pellet from a 1-l culture was resuspended in 20 ml buffer D (8 M urea, 100 mM phosphate, 10 mM Tris, pH 8.0) and stirred for 1 h to lyse cells. This solution was centrifuged at 20°C and 80 000×g for 1 h and loaded on a 5 ml Ni-NTA column and washed with 50 ml buffer D and 50 ml buffer E (buffer D at pH 6.5). P19 was refolded on the column applying a 100 ml gradient of buffer D and refolding buffer R (5 mM imidazole, 400 mM NaCl, 10 mM Tris, 100 mM phosphate, 20% glycerol) within 2 h. The column was washed again using 100 ml buffer B. The pure protein was eluted using buffer C, concentrated and dialyzed against buffer S. Optionally, the His-tag was removed to simplify some NMR spectra. In this case, the protein solution was dialyzed against buffer T (50 mM Tris-HCl, pH 7.4, 2.5 mM $CaCl_2$, 100 mM KCl) and 5 units of thrombin per mg protein was added and incubated for 24 h at 8°C. The removal of His-tag was complete. After digestion, the solution was dialyzed against buffer S. Thrombin was from human plasma and highly purified (T3010, Sigma, Deisenhofen, Germany).

2.3. Conditions for NMR samples

Samples for NMR typically contained 0.5–0.8 mM protein dissolved in buffer S (see above), 90% H_2O/10% D_2O at pH 6.9. Several sample conditions were tested to optimize for line width and solubility and to prevent aggregation. A pH titration was performed by adding minute amounts of 1 N HCl or 1 N NaOH. At four different pH values (6.5, 6.9, 7.5 and 8.4) each time a 1-D spectrum was recorded to estimate the line width and a HSQC spectrum (see NMR spectroscopy below) was recorded to check the resonances for chemical shift behavior. The optimal recording temperature was determined by increasing the temperature from 17°C to 32°C in 2°C intervals. The line width should be narrowed at higher temperatures, but this beneficial effect was offset by a strong tendency to aggregate at higher temperatures. Because of the finding that p19 is prone to aggregation, 1-D spectra were recorded in the presence of CHAPS [26] (Sigma) and $CaCl_2$ (30 mM and 60 mM). There were no dramatic changes in the case of CHAPS and almost complete precipitation of the protein upon adding $CaCl_2$. Also, a stepwise dilution was performed to determine the optimal protein concentration. A 2 mM unlabeled protein sample was diluted 1:2 with buffer S directly in the NMR tube and a 1-D spectrum was recorded after removal of half of the sample volume. This was again diluted 1:2 with buffer S and so on. The same procedure was carried out on a ^{15}N/^{13}C/^{2}H-triple labeled sample. This results in the observation that p19 aggregation is strongly dependent on the protein concentration and therefore only concentrations below 1 mM are suitable for NMR; the optimal concentration of the protein was determined to be 0.5–0.7 mM. Slowly exchanging amide protons were identified by recording a series of ^{1}H-^{15}N HSQC spectra at 5°C recorded directly after addition of D_2O and after 1, 2, 4, 6, 12 and 24 h. The measurement time for the first two spectra was 30 min.

2.4. NMR spectroscopy

NMR experiments were carried out at 27°C on the Bruker DRX 600 and DMX 750 spectrometers. Both spectrometers were equipped with triple resonance probeheads and PFG accessories. The two-dimensional total correlation spectroscopy (TOCSY) was performed with the MLEV-17 sequence [27] for isotropic mixing and a spin-lock period of 25 ms. The TOCSY pulse sequence included presaturation of the water resonance for measurements in H_2O [28]. 2-D NOESY experiments [29] were recorded with a pulse sequence in which the last 90° pulse was replaced by a jump-return sequence to suppress the water resonance [28]. A gradient pulse of 1 ms at the end of the mixing time of 120 ms was also used. 2048 complex data points were acquired in the time domain t_2 with a spectral width of 15 ppm (F_2). 750 increments in t_1 with a F_1 spectral width of 9.7 ppm and 256 scans per t_1 value were added. 2-D ^{1}H-^{15}N HSQC correlation spectra were recorded using the method of Mori et al. [30] to avoid signal losses due to fast chemical exchange. For all ^{1}H-^{15}N correlations, 128 t_1 increments were acquired with a sweep width of 2100 Hz in the nitrogen dimension. The 3D ^{1}H-^{15}N NOESY-HSQC spectrum was recorded in a water-flip-back version using constructive radiation damping [31] with a mixing time of 90 ms, and with 16 scans per t_1-t_2 pair. The spectral width and number of points acquired were 11.3 ppm and 360 real points in ^{1}H(F_1), 20.6 ppm and 44 complex points in ^{15}N(F_2), and 14 ppm and 1024 complex points in ^{1}H(F_3) with the ^{1}H(F_1), ^{15}N(F_2) and ^{1}H^{N}(F_3) carrier frequencies placed at 4.73 ppm, 117.14 ppm and 4.73 ppm, respectively. Sequential assignment was performed with triple-resonance experiments using the ^{15}N/^{3}C/^{2}D-labeled p19. Modified versions of the CT-HNCA and CT-HNCO experiments [32] were acquired, using the WATERGATE sequence [33]. The differentiation between intra- and interresidual contacts in the HNCA was achieved with a HN(CO)CA [32]. A modified version of the HN(CA)CO [34] together with the HNCO [32] was used to confirm the assignment and to resolve ambiguities. In all triple resonance experiments deuterium decoupling was employed to remove the strong quadrupolar C-D coupling [35–38]. The lock was disabled during the ^{2}D-decoupling. For the 3-D ^{15}N separated H^{N}-H$^{\alpha}$ correlation spectrum HNHA, which yielded the ^{3}J(H^{N}-H$^{\alpha}$) coupling constants from the ratio of the H^{N}-H$^{\alpha}$ cross peak to the H^{N}-H^{N} diagonal peak intensity [39], the spectral width in the ^{1}H(F_2) dimension was 9.00 ppm and 80 complex points were acquired. The ^{1}H-^{15}N heteronuclear NOE measurements were carried out using the pulse sequence of [40] on a ^{15}N uniformly labeled sample. Saturation of the amide protons in the heteronuclear NOE experiment was achieved by the application of a series of 120° pulses prior to the experiment [40]. Intensities of the cross peaks were obtained from the peak heights of two independent sets of the NOE spectra. The accuracy of the NOE measurements was ±7% for well resolved peaks and ±10–20% for overlapped peaks. All 3-D spectra were processed and evaluated on SGI workstations with the software CC-NMR [41]. A single zero filling with extensive linear prediction methods in all indirectly detected dimensions was performed for the triple resonance experiments.

3. Results and discussion

3.1. Biophysical properties of p19

The p19 protein used in this study consists of residues Leu-1–Leu-165 of the human p19 sequence plus an initial methionine residue, and in the most cases an N-terminus His-tag sequence of 19 residues. p19 was a difficult protein to study by NMR because of its low solubility in water, aggregation, and a narrow dispersion of the ^{1}H^{N} chemical shifts (Fig. 1). The ^{1}H, ^{15}N and ^{13}C spectra of p19 exhibited line widths broader than those expected for a protein of 19 kDa at concentrations of 0.2–1 mM. Solubility of the protein was low in general, better at higher pH (pH 7.5, 1 mM) and decreasing

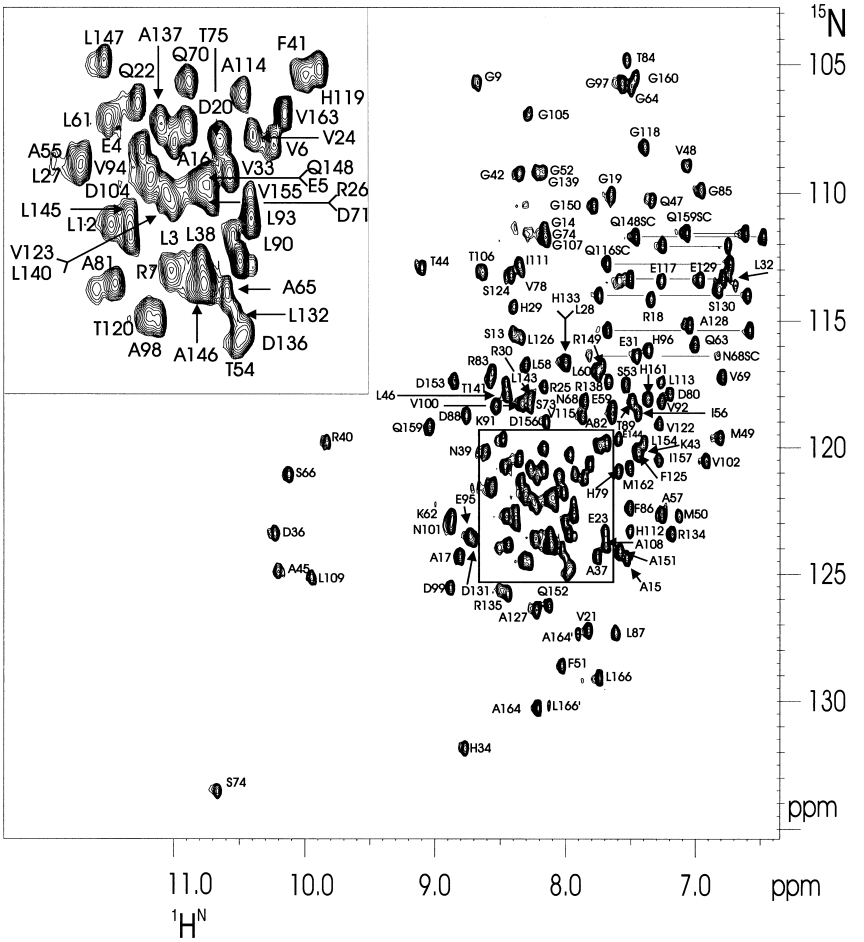

Fig. 1. ^{1}H-^{15}N HSQC spectrum of uniformly ^{15}N labeled human p19^{INK4d} recorded at pH 6.9, 27°C. Residue specific assignments of the backbone ^{1}H and ^{15}N frequencies are indicated. The horizontal lines connect the side-chain NH_2 frequencies of asparagine and glutamine residues. Cross peaks of minor conformation are marked with primes.

drastically below pH 6.5. Unfortunately, aggregation of the protein increased at higher pH (and higher concentrations). Various conditions, including changes in concentrations and pH, adding detergents, and salts were tried to reduce aggregation (see Section 2). Only lowering the concentration of the protein was found to be effective in reducing the extent of aggregation. The optimal NMR conditions for p19 were chosen as follows: pH 6.9, the protein concentration 0.7 mM in 50 mM NaCl/50 mM KCl/20 mM sodium phosphate. Under these conditions, the HNCA triple resonance experiment [42] yielded 30 correlations. ^{1}H-^{15}N TOCSY-HSQC [43] and ^{1}H-^{13}C HCCH-TOCSY [44] spectra gave even fewer transfers. Acceptable triple-resonance spectra could only be obtained after 70% deuteration of the protein. Thus, sequence specific assignments were carried out with triple-resonance spectra on the $^{15}N/^{3}C/^{2}H$-labeled protein [35–38] and sequential NOEs were extracted from the 3D ^{1}H-^{15}N NOESY-HSQC [31] spectrum recorded on the ^{15}N-labeled p19. The assignment frequently turned out to be ambiguous. Crucially helpful were HSQC spectra of ^{15}N selectively amino acid [24] labeled p19 and ^{14}N reverse amino acid labeled samples, the latter obtained from the ^{15}N minimal media supplemented with one or two unlabeled amino acid. Spin systems were identified mostly by residue specific labeling. A complete list of assignments is available from the authors. Approximately 95% of the ^{15}N, ^{13}C and ^{1}H backbone and 60% of the ^{1}H side-chain resonances have been assigned.

3.2. Conformational stability of p19

In general NOESY spectra of p19 exhibited a relatively small number of long-range NOEs for the protein of its size and several residues even showed no sequential NOEs at all. For example, no sequential, medium- or long-range NOEs were observed for residues Arg-25–His-29, Ala-45–Leu-46, and Ile-111. The Arg-25–His-29 residues could still be identified as α-helical as they exhibited significantly downfield-shifted $^{13}C^{\alpha}$, which is typical of a helical structure; also, vicinal coupling constants ($^{3}J_{NH,H\alpha}$) were consistent with those in an α-helix (Fig. 2).

In order to check whether this paucity of the NOE data could be ascribed to the protein flexibility, a 2-D ^{1}H-^{15}N heteronuclear NOE experiment [40,45] was carried out on the ^{15}N-labeled p19. The experimental ^{15}N NOE values are plotted against amino acid sequence in Fig. 3. Quantitative NOE measurements were possible for 147 residues, with an average value of 0.83. The heteronuclear ^{15}N NOE data of p19 indicated that most of the protein backbone existed in a structure of limited conformational flexibility on a picosecond time scale, with any motions faster than the rate of overall tumbling (in nanoseconds) of small magnitude [46–48]. The

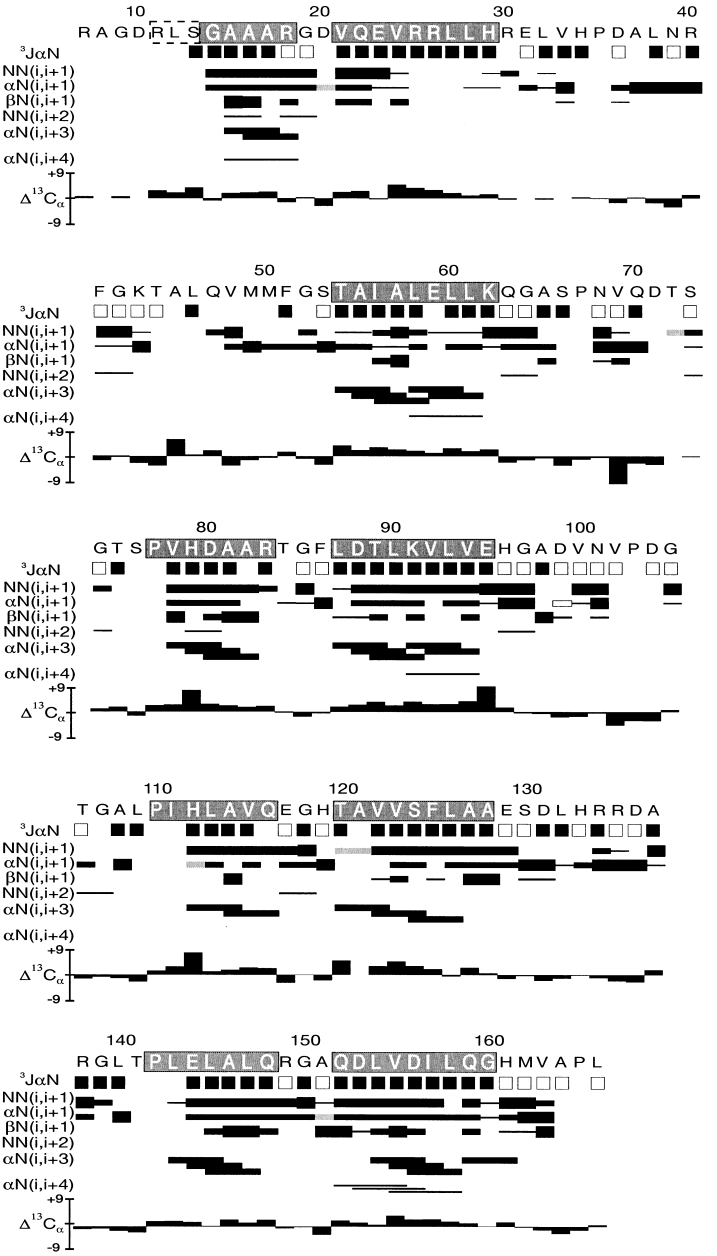

Fig. 2. Summary of the short-range (i−j < 5) NOEs, $^{3}J(H^{N}\text{-}H^{\alpha})$ coupling, and variation of $^{13}C^{\alpha}$ chemical shifts from random coil values for $p19^{INK4d}$. The NOEs, classified as weak, medium, or strong, are represented by the heights of the bars. NOEs that were uncertain because of spectral overlap are indicated by gray bars. Residues 81, 82, 93, 94, 95, 102, 109, 113, 114, 115, 124, 126, 127, and 159 showed slowly exchanging amide hydrogens that did not completely exchange for ^{2}H after 2 h at 5°C. For $^{3}J(H^{N}\text{-}H^{\alpha})$ coupling constants, small couplings (< 5 Hz) are marked with filled squares and large couplings (> 7 Hz) are represented with open squares. Boxed regions (gray shaded) represent α-helices. The amino acid sequence of p19 is divided into the five ankyrin repeats which were aligned with each other to match sequence and structurally equivalent residues. Residues 1–6 are not shown as they do not belong to the ankyrin repeat domains and were disordered in solution.

exceptions were C-terminal residues 164–166, which exhibited NOEs close to zero or negative thereby indicating significant rapid motion in this fragment of the protein backbone. Combined with the $^{3}J_{NH-H\alpha}$ coupling constants of 7 Hz [49], these data indicate that these residues formed a random conformation. No NOE data could be extracted for residues 1–3 and 8–11. However, residues 1–6 are also expected to be in the random conformation; they are close to an unstructured His-tag and include flexible residues 4 and 6 with small NOE values. In addition, residues Ala-164 and Leu-166, flanking Pro-165, showed the presence of minor and major conformations in ratio 1:4.5, respectively, slowly exchanging with each other. There were also a few residues in p19 that displayed ^{15}N NOE values characteristic of increased flexibility (^{15}N NOEs more than 25% smaller than the average value which has an error of ± 7%) [46–48]. These residues were 68, 69 and 129. All these residues were located at the ends of ankyrin repeats. Excluding trivial cases of the N- and C-terminal residues discussed above, there was however no evident correlation between residues that showed the presence of this increased flexibility and lack of proton-proton NOEs. Most probably therefore, the residues that lack proton-proton NOEs are on the solvent

exposed surface of the protein too far away from the main body of the molecule to give rise to NOE contacts.

3.3. Secondary structure and topology of ankyrin-like repeats

An overview of the observed medium-range backbone NOEs is shown in Fig. 2. These NOEs, mostly identified from the 3-D ^{15}N-resolved [^{1}H,^{1}H]-NOESY-HSQC spectra, are the basis for the determination of the secondary structure elements in proteins [49]. Short distances characteristic for α-helices, comprising $H^N(i)$-$H^N(i+1)$, $H^N(i)$-$H^N(i+2)$, $H^\alpha(i)$-$H^N(i+3)$ and $H^\alpha(i)$-$H^N(i+4)$ were found in the NOESY spectra. Additionally, chemical shifts of backbone atoms ($^{13}C^\alpha$, $^{13}C^O$ and $^1H^\alpha$) were used to predict secondary structures present in the protein sequence [50,51]. It can be seen from Fig. 2 that p19 is a highly α-helical protein with a striking topology which consists of five almost equally spaced helix-turn-helix segments between residues 14–30, 54–62, 77–95, 110–128, and 142–160. With the exception of the second segment (residues 54–62), each segment is 16–19 residues long and has a short turn located between residues 5–7 and 8–11. The results of an H/D amide exchange experiment also corroborated with the observed secondary structure elements. Slowly exchanging amide protons were observed for residues 81, 82, 93, 94, 95, 113, 114, 115, 124, 126, 127 and 159, all of them located at the C-terminal parts of the helices; additionally residues 102 and 109 were also in slow exchange. The pattern of NOEs, chemical shifts of backbone atoms $^{13}C^\alpha$ and $^1H^\alpha$, and large $^3J_{NH,H\alpha}$ coupling constants indicated that the turns occupied the β-region of φ-ψ space. The helix-turn-helix structures, which are displaced slightly toward the N-terminus from the center of an ankyrin repeat, constitute the core of ankyrin repeats [20]. It is worth stressing that the present NMR data unequivocally showed absence of the first helix in the second ankyrin repeat. Involvement of this segment in the formation of a hydrophobic core of the protein could be one possible explanation for its unusual feature. The presence of several long-range NOE contacts, mainly linking the ring protons of Phe-86 to Phe-51 and Phe-125, and linking the ring protons of Phe-86 to the H^α protons of Gly-52, indicated the existence of a hydrophobic patch in this region.

All β-turns in the helix-turn-helix segments have a central glycine residue flanked by two residues in β-conformations.

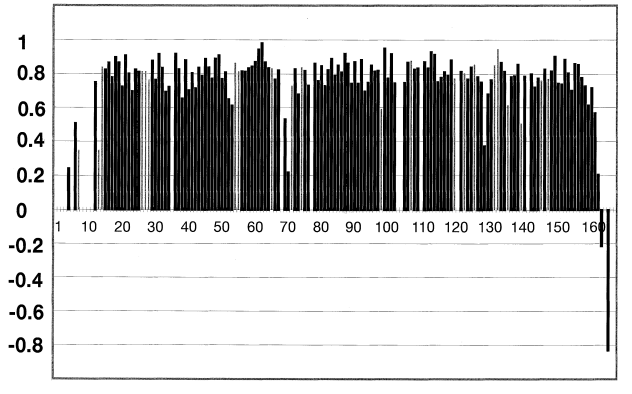

Fig. 3. Plot of the ^{15}N heteronuclear NOE as a function of the residue number for p19^{INK4d} at 27°C. Residues for which no results are shown correspond either to proline residues or to residues for which the relaxation data could not be extracted. Stippled gray bars mark residues which were overlapped (see text).

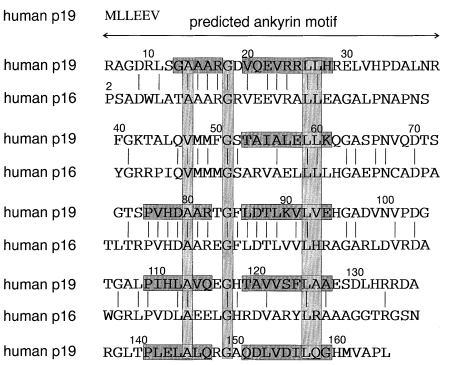

Fig. 4. Structural and sequence alignment of p19^{INK4d} and p16^{INK4a}. The structurally equivalent residues are marked in gray. Boxed regions (gray shaded) represent α-helices.

Thus, our experimental data confirm nicely the prediction of the secondary structure of ankyrin repeats [20,52], which indicated that a typical ankyrin repeat should have an eight residue long hydrophobic α-helix, starting at residue 16, preceded by a Gly containing β-turn. Based on the structural and sequence alignment of ankyrin repeats in p19 (Figs. 2 and 4), it can be seen that there is also a high conservation of some residues in the ankyrin helices. Ala at position 8 in the first helix and Leu-Leu(Val) at positions 17–18 of the second helix are highly conserved among all ankyrin repeats of p19. We predict also that the location of the helix-turn-helix structures found in p19 should be general for other members of the INK4 family. An example of such a prediction is provided in Fig. 4 with a structural and sequence alignment of p19^{INK4d} and p16^{INK4a}.

Acknowledgements: We thank Tim Mather for stimulating discussions. This work was supported by a fellowship to W.K. from the Verband der Chemischen Industrie.

References

[1] Serrano, M., Hannon, G.J. and Beach, D. (1993) Nature 366, 704–707.
[2] Sherr, C.J. and Roberts, J.M. (1995) Genes Dev. 9, 1149–1163.
[3] Hunter, T. and Pines, J. (1994) Cell 79, 573–582.
[4] Weinberg, R.A. (1995) Cell 81, 323–330.
[5] Quelle, D.E., Ashmun, R.A., Hannon, G.J., Rehberger, P.A., Trono, D., Richter, H., Walker, C., Beach, D., Sherr, C.J. and Serrano, M. (1995) Oncogene 11, 635–645.
[6] Hirai, H., Roussel, M.F., Kato, J., Ashmun, R.A. and Sherr, C.J. (1995) Mol. Cell. Biol. 15, 2672–2681.
[7] Guan, K., Jenkins, C.W., Li, Y., Nichols, M.A., Wu, X., O'Keefe, C.L., Matera, A.G. and Xiong, Y. (1994) Genes Dev. 8, 2939–2952.
[8] Koh, J., Enders, G.H., Dynlacht, B.D. and Harlow, E. (1995) Nature 375, 506–510.
[9] Lukas, J., Parry, D., Aaggard, L., Mann, D.J., Bartkova, J., Straus, M., Peters, G. and Bartek, J. (1995) Nature 375, 503–506.
[10] Medema, R.H., Herrera, R.E., Lam, F. and Weinberg, R.A. (1995) Proc. Natl. Acad. Sci. USA 92, 6289–6293.
[11] Serrano, M., Gomez-Lahoz, E., DePinho, R.A., Beach, D. and Bar-Sagi, D. (1995) Science 267, 249–252.
[12] Kamb, A., Gruis, N.A., Weaver-Feldhaus, J., Liu, Q., Harshman, K., Tavitigian, S.V., Stockkert, E., Day III, R.S., Johnson, B.E. and Skolnick, M.H. (1994) Science 264, 436–440.
[13] Nobori, N., Miura, K., Wu, D.J., Lois, A., Takabyashi, K. and Carson, D.A. (1994) Nature 368, 753–756.
[14] Hannon, G.J. and Beach, D. (1994) Nature 371, 257–161.
[15] Chan, F.K.M., Zhang, J., Cheng, L., Shapiro, D.N. and Winoto, A. (1995) Mol. Cell. Biol. 15, 2682–2688.
[16] Guan, K., Jenkins, C.W., Li, Y., O'Keefe, C.L., Noh, S., Wu, X.,

Zariwala, M., Matera, A.G. and Xiong, Y. (1996) Mol. Biol. Cell 7, 57–70.
[17] Okuda, T., Hirai, H., Valentine, V.A., Shurtleff, S.A., Kidd, V.J., Lahti, J.M., Sherr, C.J. and Downing, J.R. (1995) Genomics 29, 623–630.
[18] Merlo, A., Herman, J.G., Mao, L., Lee, D.J., Gabrielson, E., Burger, P.C., Baylin, S.B. and Sidransky, D. (1995) Nature Med. 7, 686–692.
[19] Sheaff, R.J. and Roberts, J.M. (1995) Curr. Biol. 5, 28–31.
[20] Bork, P. (1993) Proteins 17, 363–374.
[21] Xiong, Y., Hannon, G., Zhang, H., Casso, D., Kobayashi, R. and Beach, D. (1993) Nature 366, 701–704.
[22] Vieira, J. and Messing, J. (1982) Gene 19, 259–268.
[23] Sambrook, J., Fritsch, E.F. and Maniatis, T. (1989) Molecular Cloning: A Laboratory Manual, 2nd edn., Cold Spring Harbor Laboratory Press, Cold Spring Harbor, NY.
[24] Muchmore, D.C., McIntosh, L.P., Russell, C.B., Anderson, D.E. and Dahlquist, T.W. (1989) Methods Enzymol. 177, 44–73.
[25] Hoffman, D.W. and Spicer, L.D. (1991) In: Techniques in Protein Chemistry II (Villafranca, J.J., Ed.), pp. 409–419. Academic Press, San Diego, CA.
[26] Anglister, J., Grzesiek, S., Ren, H., Klee, C.B. and Bax, A. (1993) J. Biomol. NMR 3, 121–126.
[27] Bax, A. and Davis, D.G. (1985) J. Magn. Reson. 65, 355–360.
[28] Guèron, M., Plateau, P. and Decorps, M. (1991) Prog. NMR Spectrosc. 23, 135–209.
[29] Jeener, J., Meier, B.H., Bachman, P. and Ernst, R.R. (1979) J. Chem. Phys. 71, 4546–4553.
[30] Mori, S., Abeygunawardana, C., Johnson, M.N. and van Zijl, P.C.M. (1995) J. Magn. Reson. B 108, 94–98.
[31] Jahnke, W., Baur, M., Gemmecker, G. and Kessler, H. (1995) J. Magn. Reson. B 106, 86–88.
[32] Grzesiek, S. and Bax, A. (1992) J. Magn. Reson. 96, 432–440.
[33] Sklenář, V., Piotto, M., Leppik, R. and Saudek, V.J. (1993) Magn. Reson. A 102, 241–245.
[34] Clubb, R.T., Thanabal, V. and Wagner G. (1992) J. Magn. Reson. 97, 213–217.
[35] Grzesiek, S., Anglister, J., Ren, H. and Bax, A. (1993) J. Am. Chem. Soc. 115, 4369–4370.
[36] Shan, X., Gardner, K.H., Muhandiram, D.R., Rao, N.S., Arrowsmith, C.H. and Kay, L.E. (1996) J. Am. Chem. Soc. 118, 6570–6579.
[37] Nietlispach, D., Clowes, R.T., Broadhurst, R.W., Ito, Y., Keeler, J., Kelly, M., Ashurt, J., Oschkinat, H., Domaille, P.J. and Laue, E.D. (1996) J. Am. Chem. Soc. 118, 407–415.
[38] Venters, R.A., Metzler, W.J., Spicer, L.D., Mueller, L. and Farmer III, B.T. (1996) J. Am. Chem. Soc. 117, 9592–9593.
[39] Vuister, G.W. and Bax, A. (1993) J. Am. Chem. Soc. 115, 7772–7777.
[40] Farrow, N.A., Muhandiram, R., Singer, A.U., Pascal, S.M., Kay, C.M., Gish, G., Shoelson, S.E., Pawson, T., Foreman-Kay, J.D. and Kay, L.E. (1994) Biochemistry 33, 5984–6003.
[41] Cieslar, C., Ross, A., Zink, T. and Holak, T.A. (1993) J. Magn. Reson. B 101, 97–101.
[42] Ikura, M., Kay, L.E. and Bax, A. (1990) Biochemistry 29, 4659–4667.
[43] Marion, D., Driscoll, P.C., Kay, L.E., Wingfield, P.T., Bax, A., Gronenborn, A.M. and Clore, G.M. (1989) Biochemistry 28, 6150–6156.
[44] Kay, L.E., Xu, G.-Y., Singer, A.U., Muhandiram, D.R. and Foreman-Kay, J.D. (1993) J. Magn. Reson. B 101, 333–337.
[45] Kay, L.E, Torchia, D.A. and Bax, A. (1989) Biochemistry 28, 8972–8979.
[46] Clore, G.M., Driscoll, P.C., Wingfield, P.T. and Gronenborn, A.M. (1990) Biochemistry 27, 7387–7401.
[47] Clubb, R.T., Omichinski, J.G., Sakaguchi, K., Appella, E., Gronenborn, A.M. and Clore, G.M. (1995) Protein Sci. 3, 855–862.
[48] Zink, T., Ross, A., Lüers, K., Cieslar, C., Rudolph, R. and Holak, T.A. (1994) Biochemistry 33, 8453–8463.
[49] Wüthrich, K. (1986) NMR of Proteins and Nucleic Acids. Wiley, New York.
[50] Spera, S. and Bax, A. (1991) J. Am. Chem. Soc. 113, 5490–5492.
[51] Wishart, D.S., Sykes, B.D. and Richards, F.M. (1991) J. Mol. Biol. 222, 311–333.
[52] Gay, N.J. and Ntwasa, M. (1993) FEBS Lett. 335, 155–160.